Lecture 8&9: *Pulsar Wind Nebulae (Plerions)* and *Gamma Ray Loud Binary Systems*

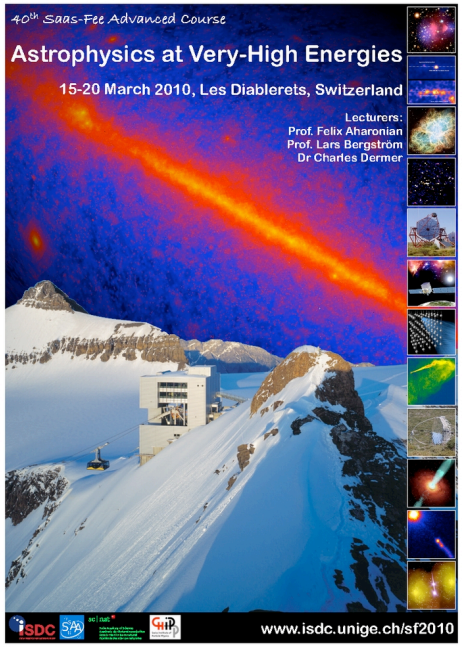

F.A. Aharonian, *DIAS (Dublin)* & *MPIK (Heidelberg)*

Les Diablerets, March 15-20, 2010

Relativistic winds and Jets in Astrophysics

- nonthermal phenomena in *Pulsars, μQSOs, AGN, GRBs* are linked, in one way or another, to relativistically moving plasmas (bulk motions)

- relativistic outflows in forms of *winds* and *jets* are tightly coupled with compact objects: *Neutron Stars and Black Holes*

- relativistic outflows as effective accelerators of *Cosmic Rays* are, most likely, the only realistic sites for acceleration of 10^{20} eV CRs

Relativistic outflows as extreme accelerators

distinct feature of relativistic outflows: effective particle acceleration at different stages of their development

close to the central engine (base of the jet)
during propagation on large scales,
at the jet (wind) termination

the theory of relativistic jets – very complex and not (yet) fully understood – all aspects (MHD, electrodynamics, shock waves, particle acceleration) contain many problems and uncertainties, but it is likely that these are the best accelerators in the Universe with maximum (theoretically possible) acceleration rate: ηqBc with $\eta \sim 1$.

Crab Nebula – an extreme accelerator

a unique PWNe

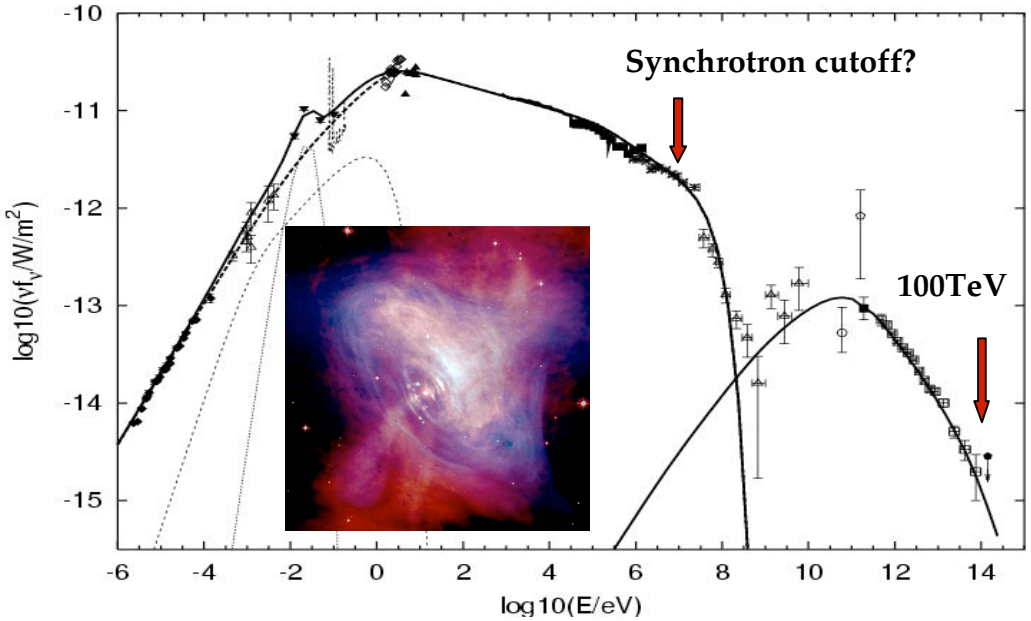

Standard MHD theory

cold ultrarelativistc pulsar wind terminates by a reverse shock resulting in acceleration of electrons to multi-100 TeV energies resulting in 2 non-thermal extended structures:

optical-X-γ synchrotron nebula
γ-ray inverse-Compton nebula

flux and energy spectrum are explaied if $L_e \sim 0.5 L_{rot} = 2 \times 10^{38}$ erg/s and $E_{e,max} > 100$ TeV:

$E_{e,max} = 60\,(B/1G)^{-1/2}\,\eta^{-1/2}$ TeV, where η charcterizes acceleration rate: $t_{acc} = \eta\,(R_L/c)$, $\eta > 1$

$$h\nu_{cut} = 9/4\,\alpha_f^{-1} mc^2\,\eta^{-1} = 150\,\eta^{-1}\ \text{MeV}$$

Crab: $h\nu_{cut} \sim 10$MeV: $\eta \sim 10$ => *acceleration at ~10 % of the maximum rate !*

a more model-independent estimate for η based on TeV data:

maximum energy of electrons: $E_\gamma = 100$TeV => $E_{e,max} >$ few x 100TeV ; for B=0.2 μG, $\eta < 100$

EGRET data - higher by a factor of two of IC predictions;
a need in an additional component/bremsstrahlung ?

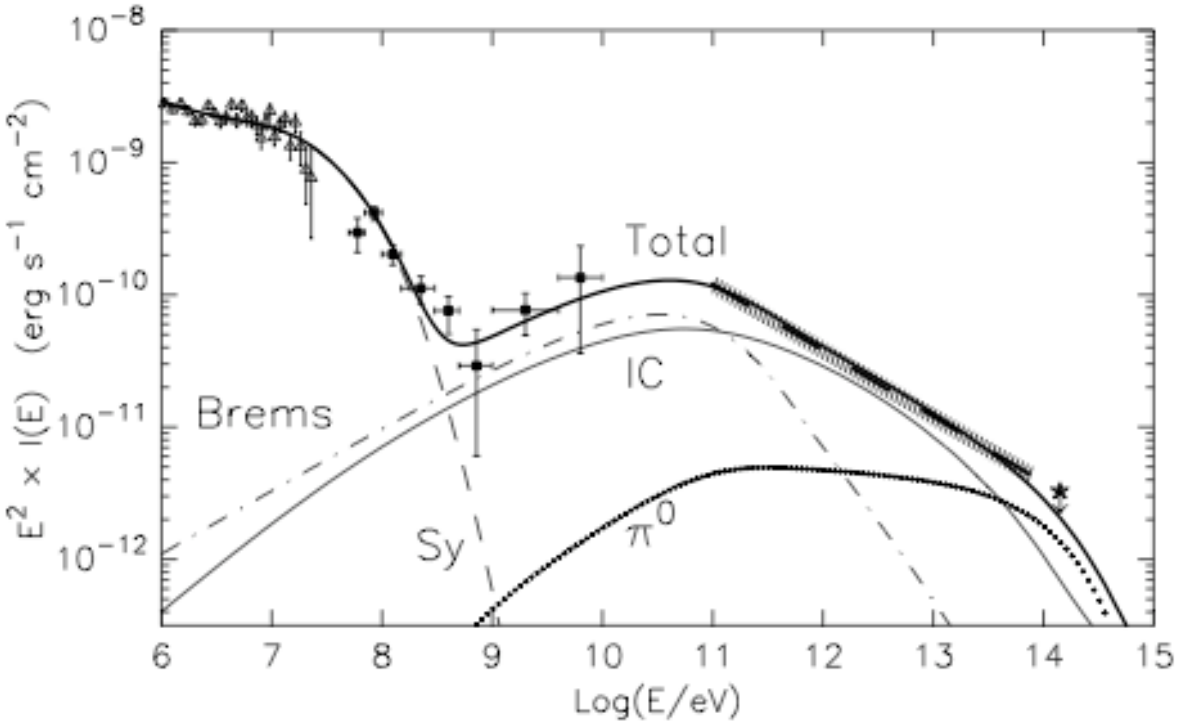

Fig. 6.17 The contributions of different γ-ray production mechanisms to the total non-thermal radiation of the Crab Nebula. The Synchrotron and IC components are the same as in Fig. 6.16. The bremsstrahlung and π^0-decay γ-ray fluxes are calculated for $n_{\rm eff} = 50\,{\rm cm}^{-3}$. (From Aharonian and Atoyan, 1998b).

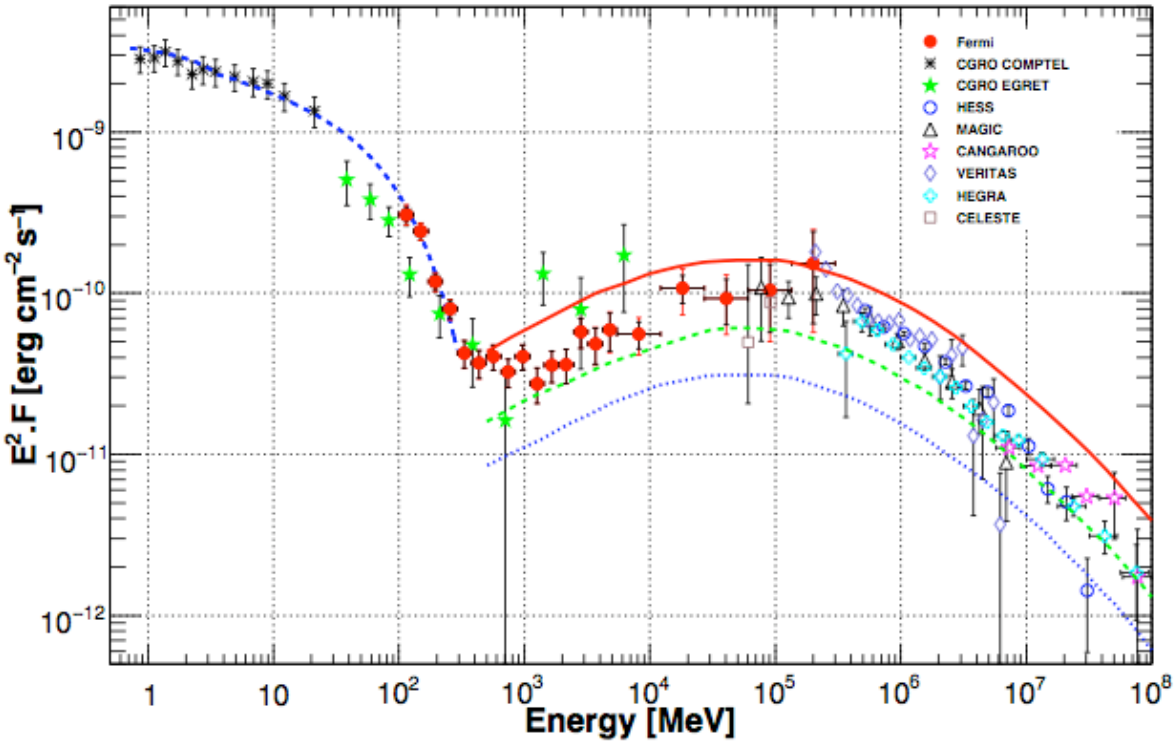

FIG. 9.— The spectral energy distribution of the Crab Nebula from soft to very high energy γ-rays. The fit of the synchrotron component, using COMPTEL nd LAT data (blue dashed line), is overlaid. The predicted inverse Compton spectra from Atoyan and Aharonian (1996) are overlaid for three different values of ıe mean magnetic field: 100 μG (solid red line), 200 μG (dashed green line) and the canonical equipartition field of the Crab Nebula 300 μG (dotted blue line). :eferences: CGRO COMPTEL and EGRET: Kuiper et al. (2001); MAGIC: Albert et al. (2008); HESS: Aharonian et al. (2006); CANGAROO: Tanimori et al. 1997); VERITAS: Celik (2007); **HEGRA:** Aharonian et al. (2004); **CELESTE:** Smith et al. (2006)

results from *Fermi* LAT - (1) confirmation of IC origin of TeV emission! no any additional component is needed; (2) good agreement with MAGIC; (3) sharp transition from Synch to IC

important tests

- Energy-dependent size 0.1 -10 TeV (***MAGIC –II and VERITAS***)
- ✓ Energy spectrum 100 MeV to 100 GeV (***GLAST***)
- Detection of a sharp cutoff around 100 TeV (***HESS***)
- Detection of γ-ray line signatures (at $E_\gamma = m_e c^2 \times G$) of the unshocked wind (***GLAST***)
- > 1 TeV neutrinos (marginally) detectable (***Ice Cube***)

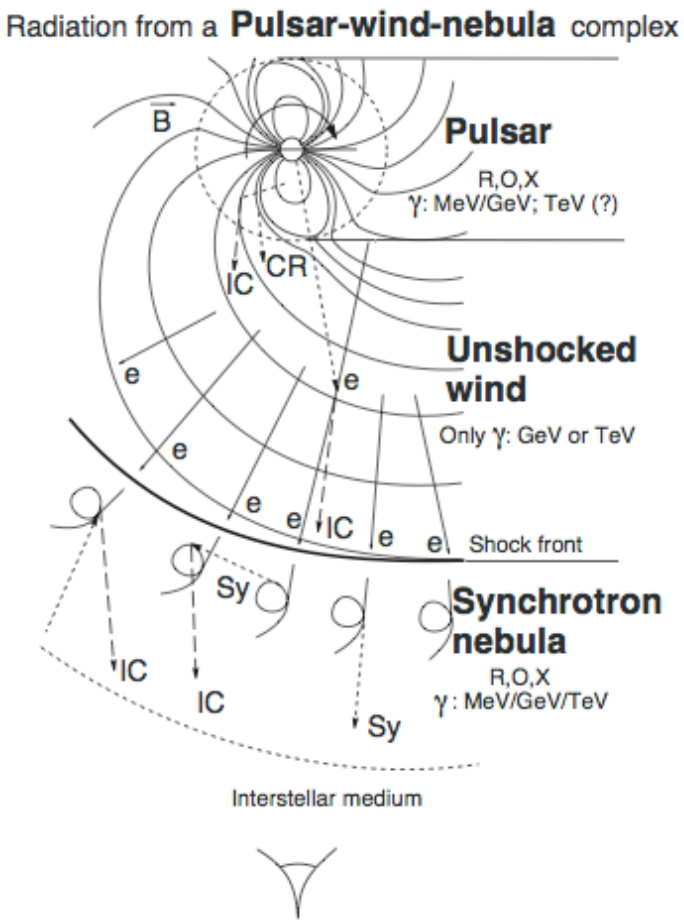

Fig. 1.8 Three regions of nonthermal radiation associated with a rotation powered pulsar: *pulsar* – magnetospheric pulsed γ-ray emission produced within the light cylinder due to the curvature, synchrotron, and inverse Compton processes; *unshocked wind* – gamma-radiation of the cold wind at GeV and TeV energies through the relativistic bulk-motion Comptonization; *synchrotron nebula* – broad-band, synchrotron and IC emission of the nonthermal nebulae (from Aharonian and Bogovalov, 2003).

Probing the “birth” place and the Lorentz factor of the Pulsar Wind

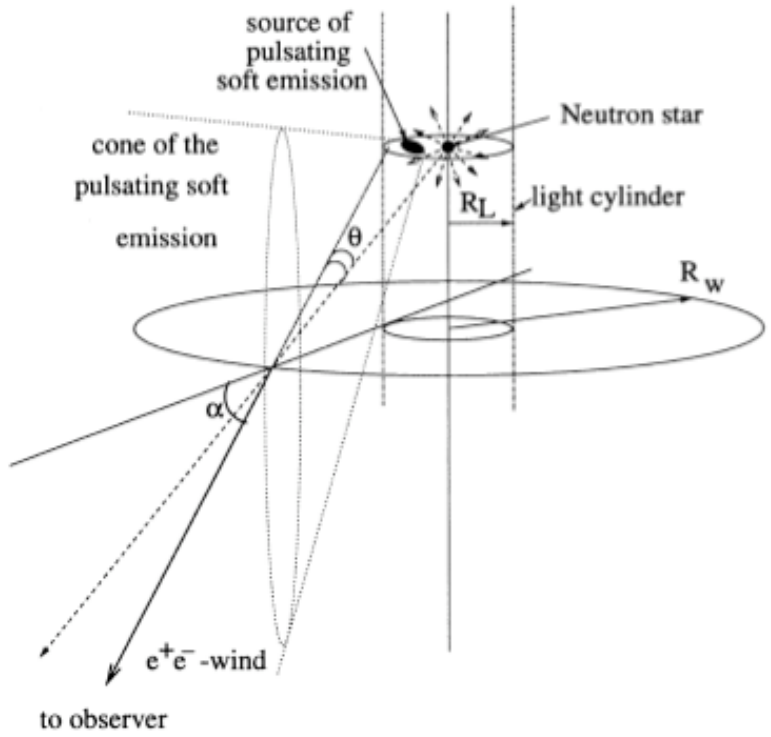

Figure 1. A sketch of the trajectories of plasma after acceleration, and the assumed position of sources of soft photons.

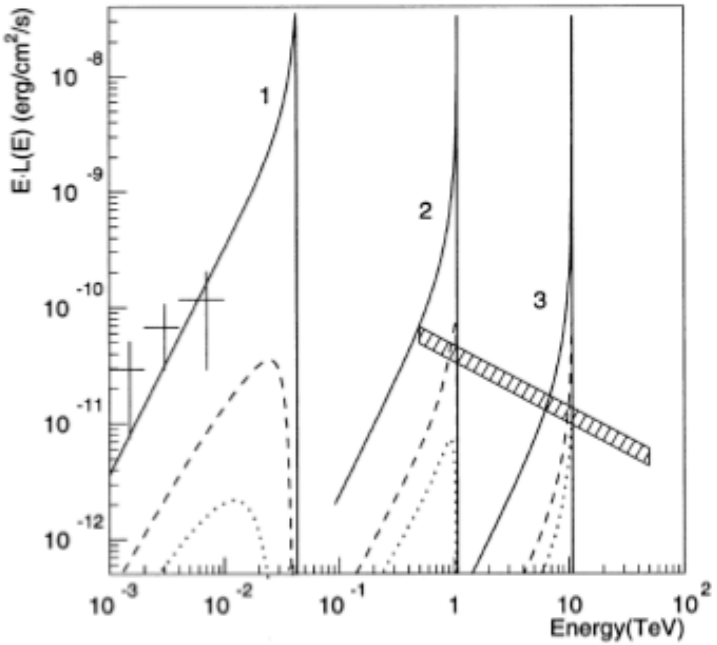

Figure 4. The spectra of IC radiation of the wind illuminated by the thermal emission of the pulsar. It is assumed that the kinetic-energy dominated wind is formed at distances of 1 (solid), 5 (dashed) and 10 (dotted) light cylinders from the pulsar. The curves 1, 2 and 3 correspond to $\gamma_{max} = 1.2 \times 10^5$, 3×10^6 and 3×10^7. The range of observed fluxes of γ-rays in the region above 500 GeV detected by the CAT, CANGAROO, HEGRA and Whipple telescopes is shown by a shadowed region. The points with error bars below 10 GeV correspond to the unpulsed fluxes measured by EGRET.

Bogovalov&Aharonian 2000

TeV gamm-rays from other Plerions ?

Crab Nebula is a very effective accelerator
but not an effective IC γ-ray emitter

we see TeV gamma-rays from the Crab Nebula because of
very large spin-down flux

but gamma-ray flux << "spin-down flux"
because of large magnetic field

the strength of B-field also depends on the external pressure and L_{rot}

weaker magnetic field => higher gamma-ray efficiency $k \sim \min[1, (B/3\mu G)^2]$
=> detectable gamma-ray fluxes from other plerions

HESS confirms this prediction – several famous PWN already detected -
MSH 15-52, PSR 1825, Vela X, ...

* Plerions – Pulsar Driven Nebulae

There are 26 detected PWNs (out of 105 TeV sources)

Crab *(standard candle)*	Geminga
Vela X	G292.2-0.5
HESS J1356-645	Kookaburra (Rabbit)
Kookaburra (Pulsar)	MSH 15-52
HESS J1616-508	HESS J1640-465
HESS J1708-443	HESS J1718-385
HESS J1809-193	HESS J1813-178
HESS J1825-137	HESS J1833-105
HESS J1846-029	IGR J18490-0000
HESS J1912+101	HESS J1923+141
G54.1+0.3	0FGL J1958.1+2848
MGRO J2019+37 20	0FGL J2021.5+4026
Boomerang	0FGL J0631.8+1034

Source *http://tevcat.uchicago.edu/*

small B-filed - a key assumption for TeV PWNe to explain

- large TeV/X-ray ratio: $L_\gamma/L_x \sim 1(B/3\mu G)^{-2}$
- pure power-law spectra (from <<1 TeV to >> 10 TeV)
- very large size, R >> 10pc
- to explain very high gamma-ray efficiency: $L_\gamma/L_{rot} \sim 0.1$!

Kennel&Coroniti, 1984

The basic equations

$$(r/r_{\rm sh})^2\,(n/n_0)\,u = 1$$

$$\frac{(w/w_0)\,\gamma}{(n/n_0)} + \frac{(B/B_0)^2}{\gamma\,(n/n_0)} = 1+\sigma$$

$$\frac{(B/B_0)}{(r/r_{\rm sh})\gamma(n/n_0)} = \sigma^{1/2}$$

$$\frac{(w/w_0)}{(n/n_0)^{4/3}} = \frac{2}{3}(1-\sigma)$$

w is enthalpy (per unit of volume); p is pressure; B is magnetic field; n is particle density; σ (is assumed to be $\ll 1$) is magnitization of the pulsar wind; and u is radial component of 4-velocity

- Radial flow
- Toroidal B-field
- Steady flow
- Pulsar wind $\Rightarrow$ bon. conditions at termination shock
- Bon. conditions at $r \to \infty$ give $r_{\rm sh}$
- Few free parameters (e.g. σ, $r_{\rm sh}$)

small magnetic field ?

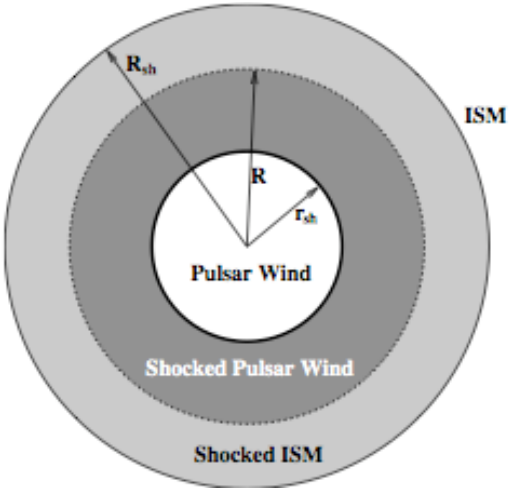

Radius of the termination shock

$$r_{\rm sh} = 5 \cdot 10^{18}{\rm cm} \left(\frac{L_{\rm SD}}{10^{37}{\rm erg/s}}\right)^{1/2} \left(\frac{p_{\rm ism}}{10^{-12}{\rm erg/cm^3}}\right)^{-1/2}$$

Size of the PWN

$$R \sim 2 \cdot 10^{20}{\rm cm} \left(\frac{L_{\rm SD}}{10^{37}{\rm erg/s}}\right)^{1/3} \left(\frac{t}{10^{5}{\rm yr}}\right)^{1/3} \left(\frac{p_{\rm ism}}{10^{-12}{\rm erg/cm^3}}\right)^{-1/3}$$

Magnetic field

$$B \sim 6 \cdot 10^{-7}{\rm G} \left(\frac{\sigma}{3 \cdot 10^{-3}}\right)^{1/2} \left(\frac{p_{\rm ism}}{10^{-12}{\rm erg/cm^3}}\right)^{1/2}$$

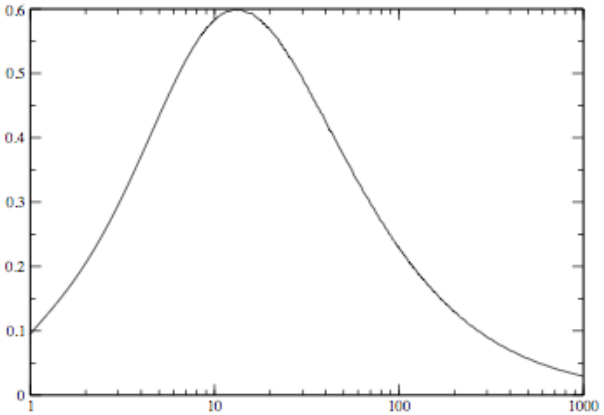

Figure 9. Strength of the B-field as a function of radial distance. The following parameters were assumed: $L_{\rm sd} = 10^{37}$ erg/s, $\sigma = 3 \cdot 10^{-3}$ and $r_{\rm sh} = 5 \cdot 10^{18}$ cm.

Gun&Rees 1974
Kennel & Coroniti 1984

HESS J1825 (PSR J1826-1334)

a standard PWNe

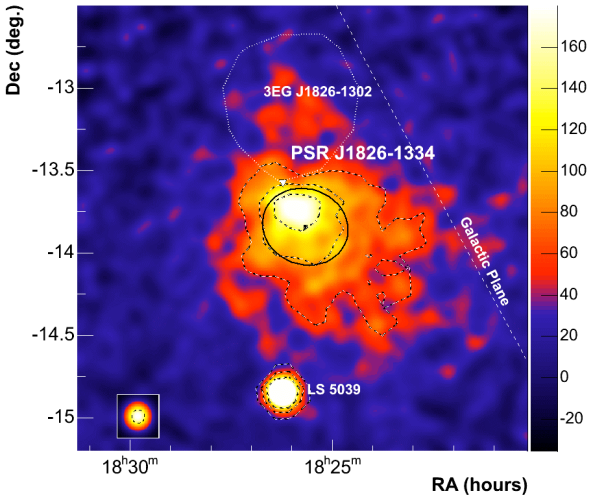

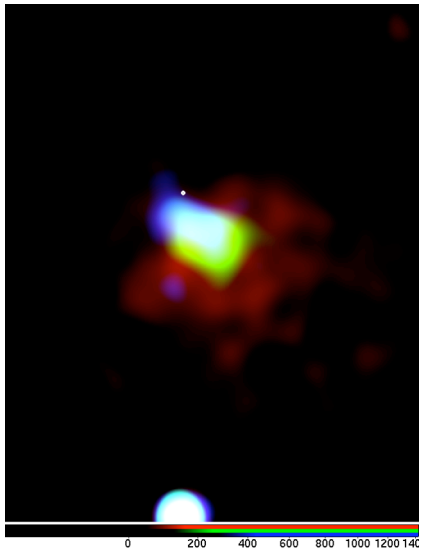

energy-dependen image !

red – below 0.8 TeV
yellow – 0.8TeV -2.5 TeV
blue – above 2.5 TeV

Pulsar's period: 110 ms, age: 21.4 kyr,
distance: 3.9 +/- 0.4 kpc

Luminosities:

spin-down: $L_{rot}= 3 \times 10^{36}$ erg/s

X: 1-10 keV $Lx=3 \times 10^{33}$ erg/s (< 5 arcmin)

γ: 0.2-40TeV $L_{\gamma}=3 \times 10^{35}$ erg/s (< 1 degree)

the γ-ray luminosity is comparable to the TeV luminosity of the Crab Nebula, while the spindown luminosity is two orders of magnitude less ! implications ?

(a) magnetic field should be significantly less than 10mG.

but even for $L_e=L_{rot}$ this condition alone is not sufficient to achieve 10 % γ-ray production efficiency (Compton cooling time of electrons on 2.7K CMBR exceeds the age of the source)

(b) the spin-down luminosity in the past was much higher.

SED of a typical PWNe with small B field

a standard PWNe

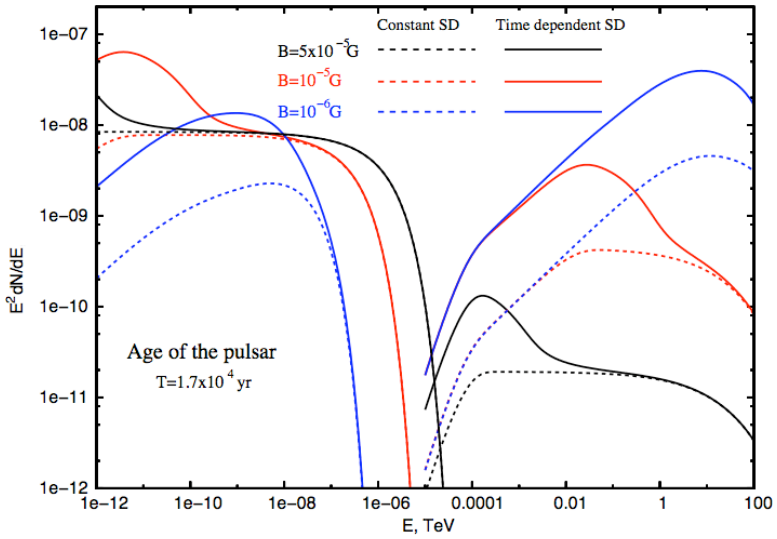

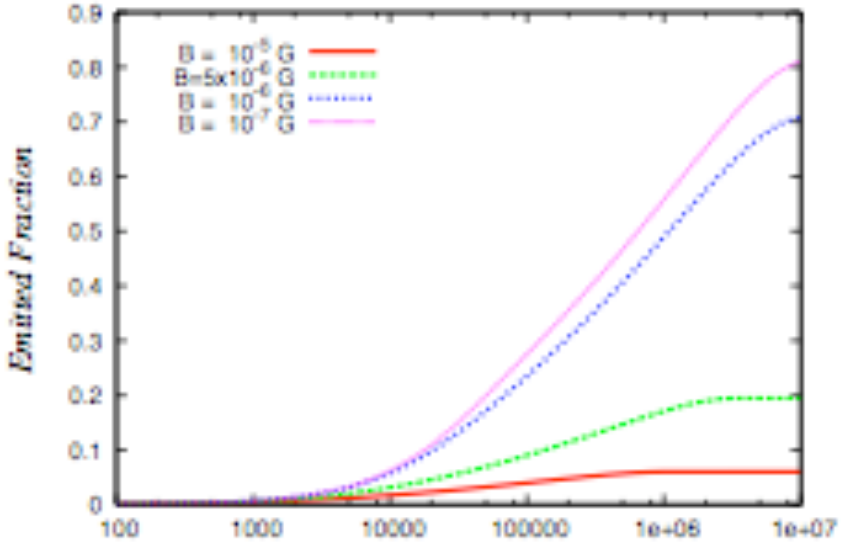

Figure 1. Fracton of energy emitted through IC channel. The target field was assumed to be CMB. The injection was assumed to be steady. We plot the ratio of luminosity injected between 100GeV and 10TeV to the injected luminosity in the relevant energy range (accounting for transition between the Klein-Nishina and the Thomson scattering regims).

$L_{rot}(t)=L_0\ (1-t/T)^{-2}$ (breaking index 3), $dN/dE\sim E^{-2.2}$; Ecut=300 TeV

MSH 15-52

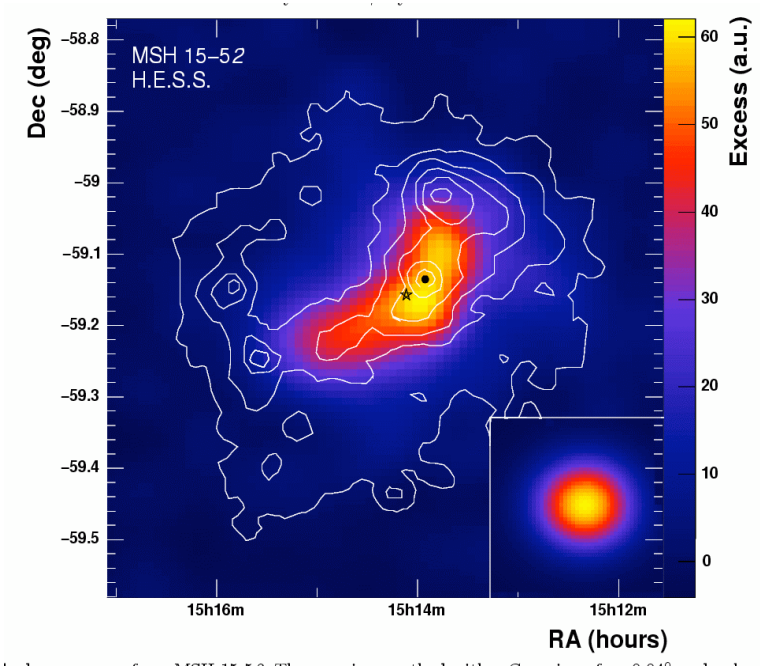

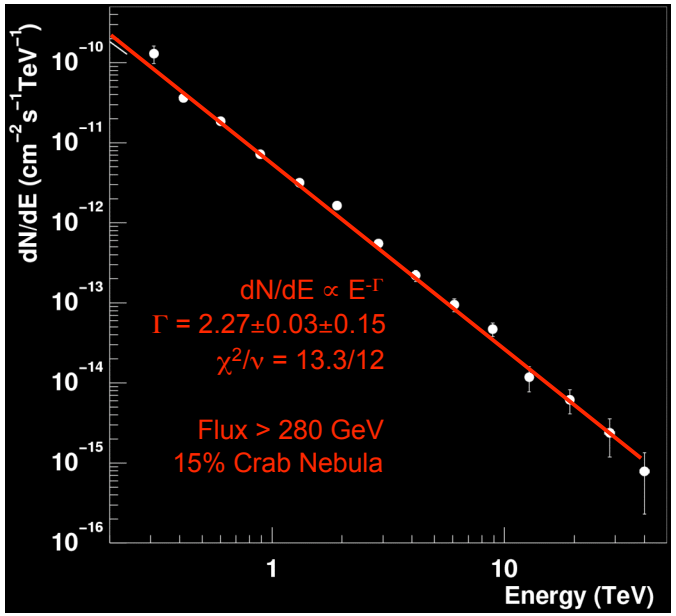

since 2.7 K MBR is the main target field, TeV images reflect spatial distributions of electrons Ne(E,x,y); coupled with synchrotron X-rays, TeV images allow measurements of B(x,y)

the energy spectrum - a perfect hard power-law with photon index Γ=2.2-2.3 over 2 decades !

cannot be easily explained by IC… (unless intense IR sources around)

hadronic (p^o-decay) origin of g-rays ?

very weak magnetic field ?

HESS J0835-456 (Vela X) – *do we see the Compton peak ?*

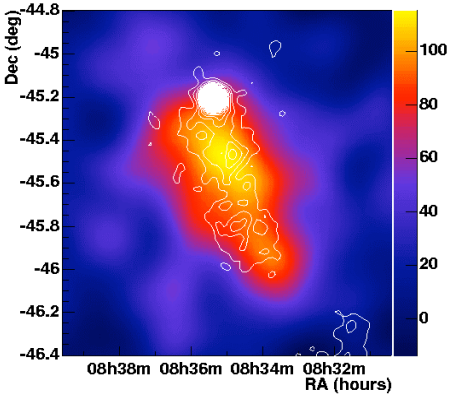

the image of TeV electrons ! (?)

spectral index α_e= 2 with a
break around 70 TeV
total energy We=2×10^{45} erg !!!

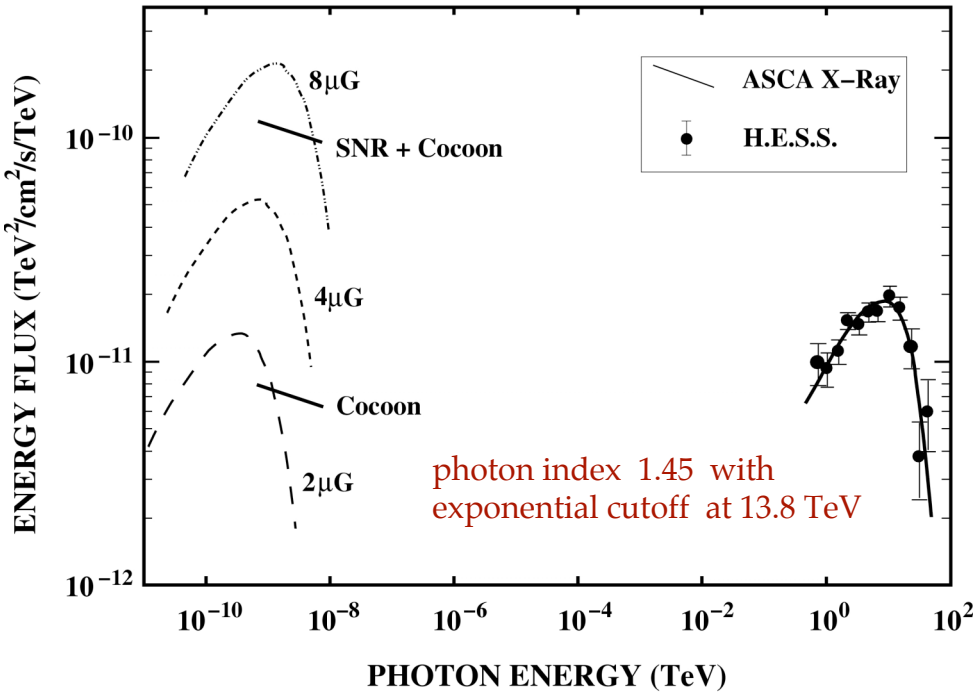

questions:

- B-field – as weak as 2 μG ?
- energy in ultrarelativistic electrons only 2×10^{45} erg ?
- integrated energy over 11kyr: >2.5×10^{48} erg – in which form the "dark energy" is released?

adiabatic losses?, 'inisible' low energy electrons? or in ultrarelativistic protons?

pulsar wind consisting of protons and nuclei* ...

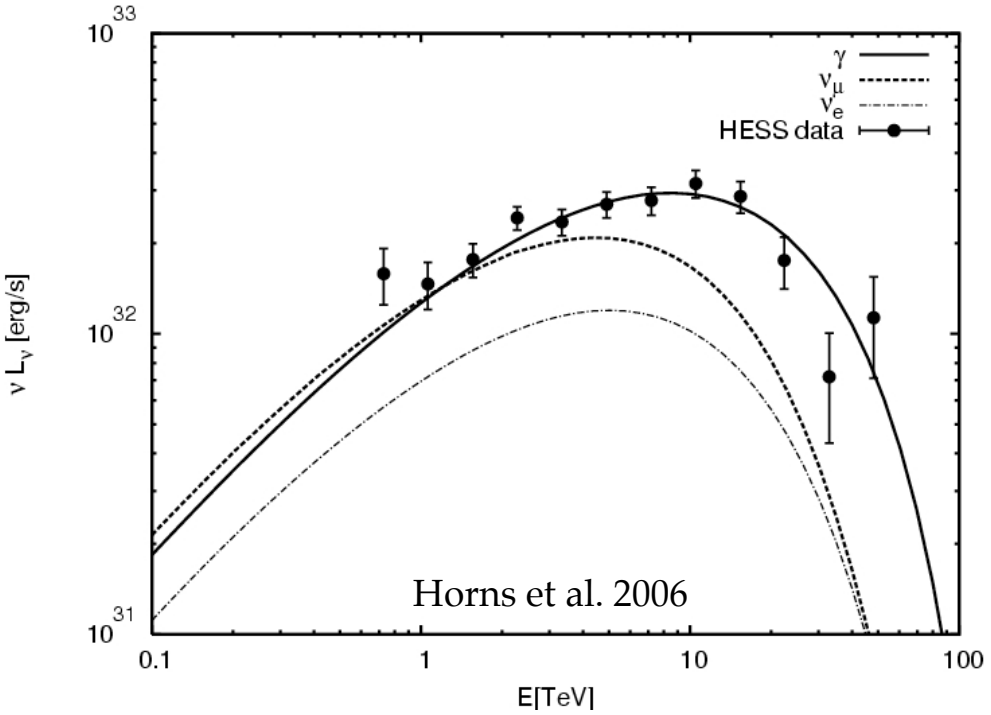

$dN_p/dE = AE^2 \exp[-(E/80\text{TeV})^2]$

$W_p = 1.3 \times 10^{49} (n/0.6\text{cm}^{-3})$ erg

total spin down energy released over the last 11kyr: 5×10^{48} – 5×10^{51} erg depending on the braking index, i.e. history of L_{rot}

even for smaller density, the energy budget is not a big issue…

but is there any need to invoke protons at all?

fluxes of TeV neutrinos are detectable by KM3NeT !

MSH-15-52 and Vela X

both are of almost same age (10kyr), same power L_{rot}, 10^{37} erg/s), and angular size, but very different luminosities, energy spectra, distances and … sizes!

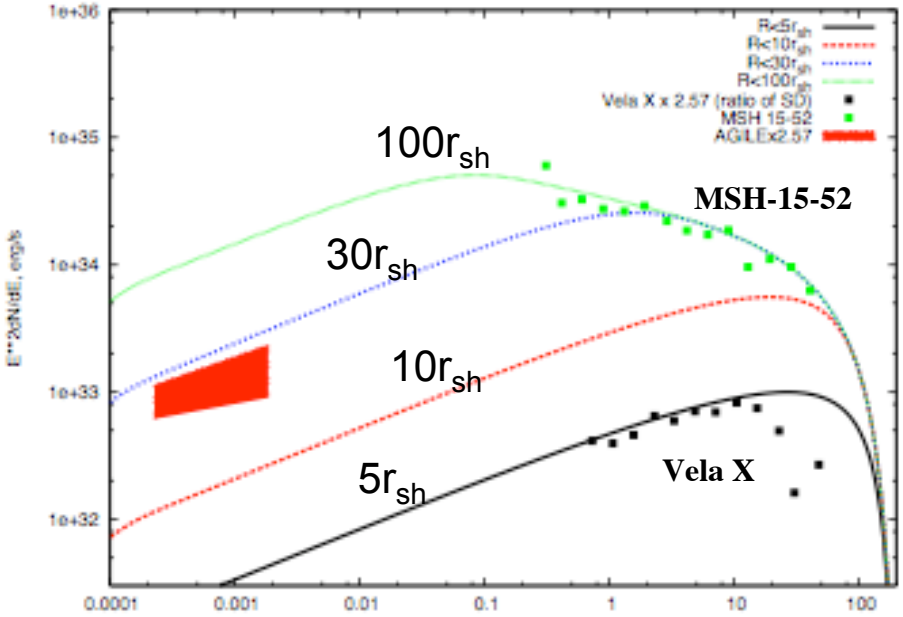

because the small distance to Vela X, we see only a very small part of the nebula => very low luminosity, but also because of quick escape of electrons from this small area - We see IC spectrum of uncooled electrons

$L=1.8\ 10^{37}$ erg/s, $r_{sh}=5\ 10^{18}$s, $\sigma=3\ 10^{-3}$, $Q(E)=E^{-2.2}\exp(-E/300\text{TeV})$

Khangulyan, FA, Bogovalov 2010

PSR1259-63 - a unique high energy laboratory

binary pulsars - a special case with strong effects associated with the optical star on both the dynamics of the pulsar wind and the radiation before and after its termination

the same 3 components - *Pulsar/Pulsar Wind/Synch.Nebula* - as in PWNe*
both the electrons of the cold wind and shocke-accelerated electrons are illuminated by optical radiation from the companion star ⟶ detectable IC γ-ray emission

"on-line watch" of the MHD processes of creation and termination of the ultrarelativistic pulsar wind, as well as particle acceleration by relativistic shock waves (?), through spectral and temporal studies of γ-ray emission

(characteristic timescales 1h or shorter !)

the target photon field is function of time, thus the only unknown parameter is B-field:

TeV electrons are cooled and and radiate in deep Klein-Nishina regime with very interesting effects on both synchrotron X-rays and IC gamma-rays

see Tavani and Arons 1997

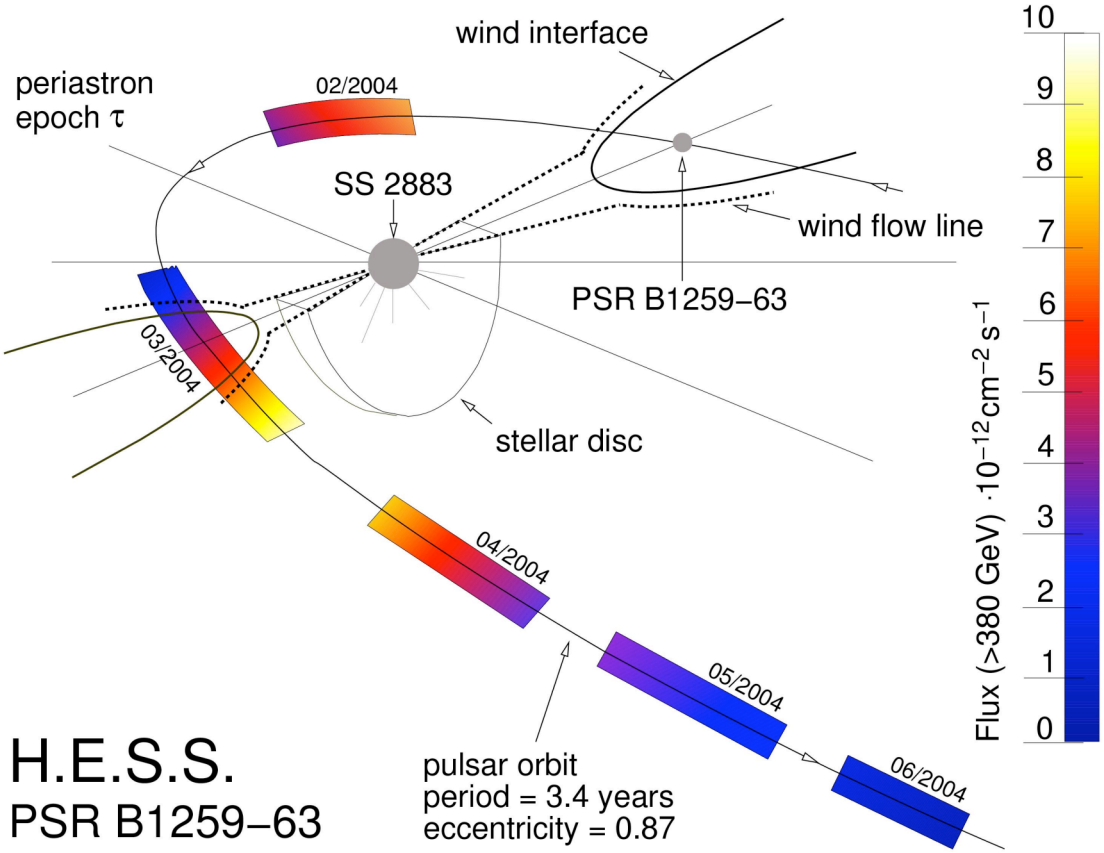

energy flux of starlight close to the periastron around **1 erg/cm^3**

B-field is estimated between **0.1 to 1 G**

predictable X and gamma-ray fluxes ?

time evolution of fluxes and energy spectra of X- and γ-rays contain unique information about the shock dynamics, electron acceleration, B(r), ...

HESS: detection of TeV γ-rays from PSR1259-63 at < 0.1Crab level several days before the periastron and 3 weeks after the periastron

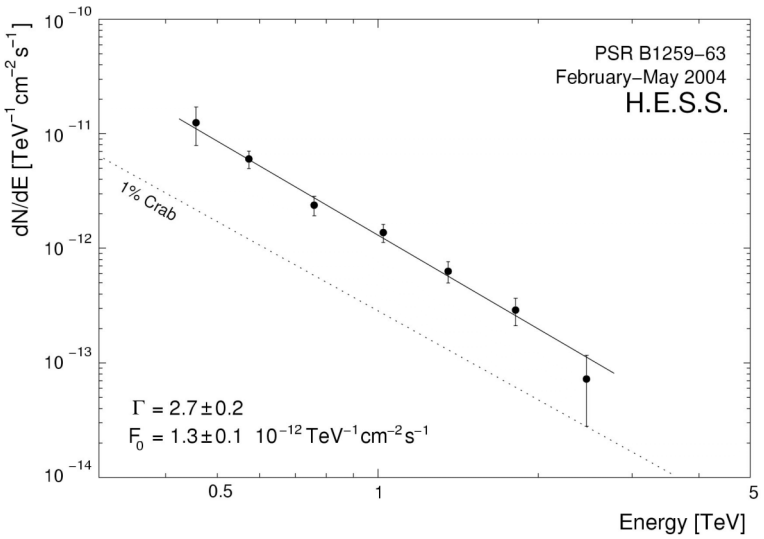

while the gamma-ray energy spectrum can be explained by IC mechanism

the lightcurve is still a puzzle

deep theoretical (in particular MHD) studies needed to understand the source

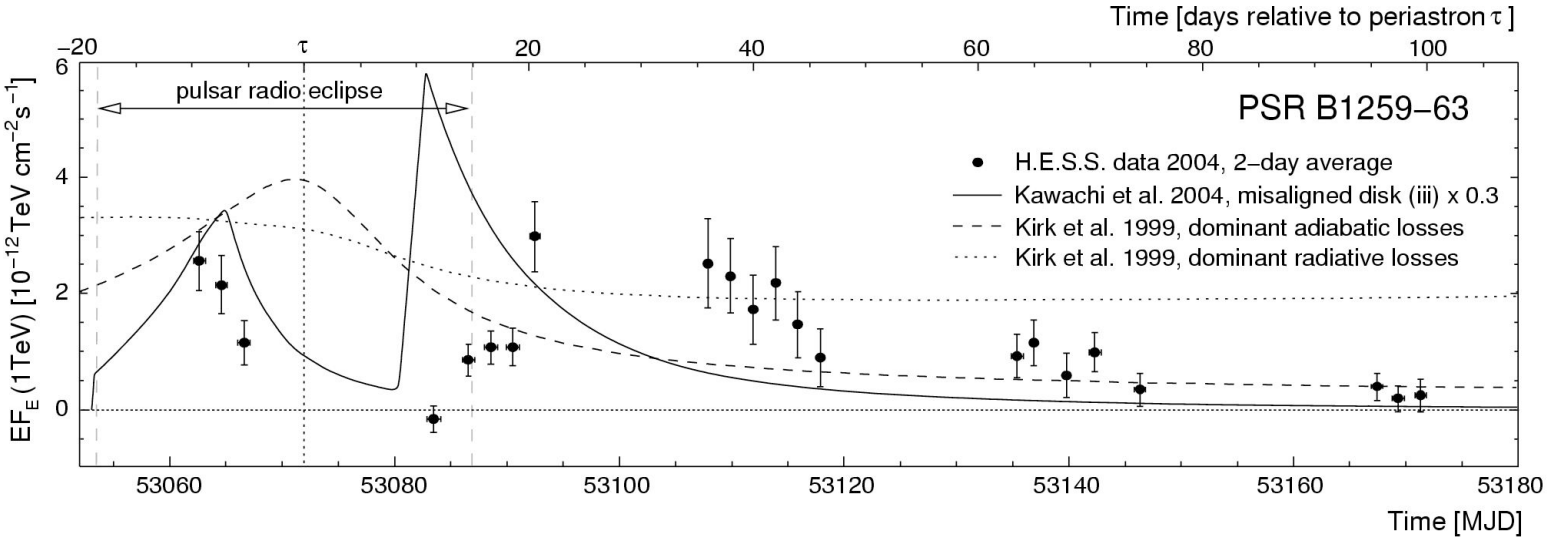

Explanation of the TeV lightcurve within the IC model:
sub-TeV cutoffs

variation of the maximum energy of electrons due to IC losses

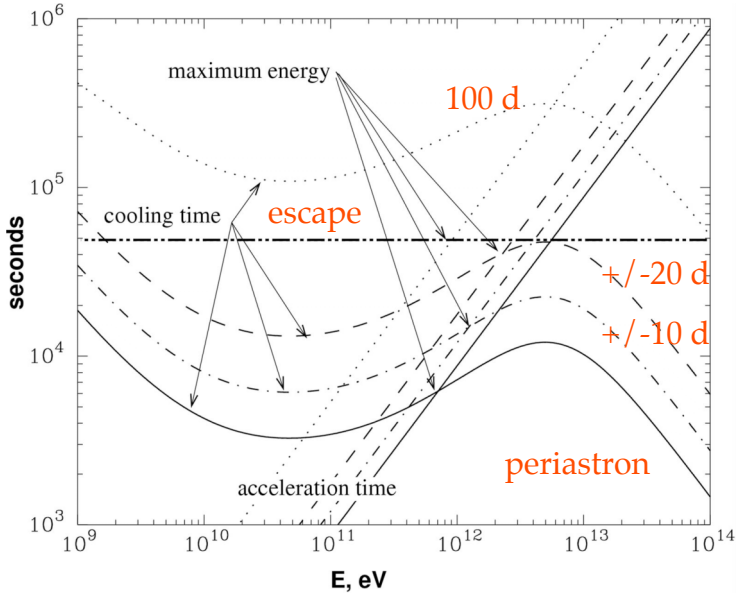

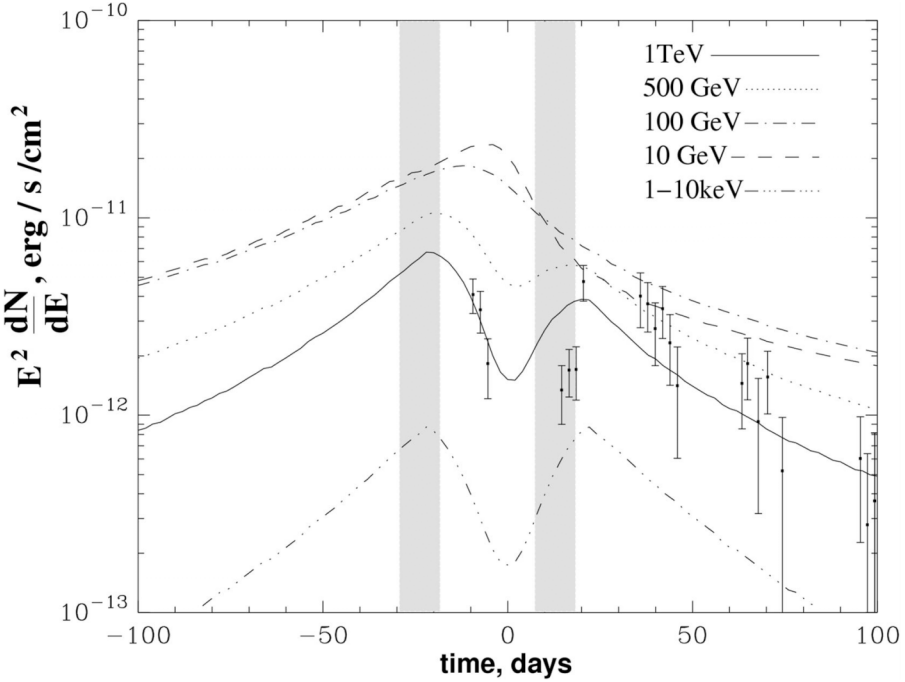

Bo=0.05 (Do/D) Gauss,
$t_{acc} = \eta\, r_L / c$; $\eta = 4 \times 10^3$

minimum at periastron at high energies,
but maximum – at low energies

Khangulyan et al. 2007

adiabatic losses?

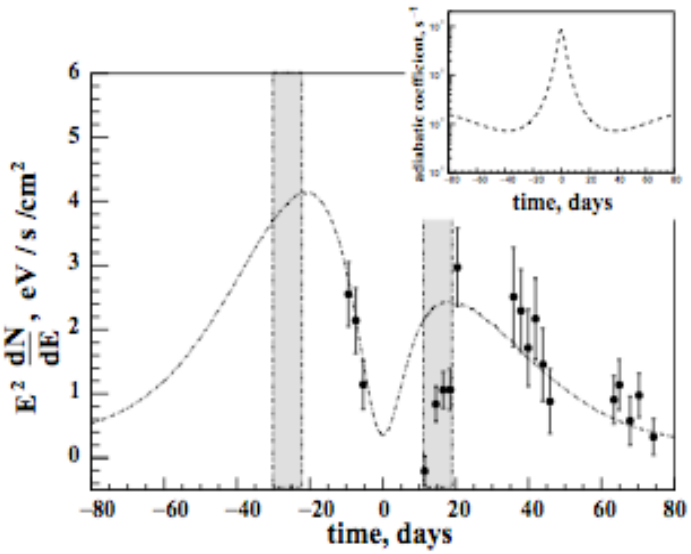

Figure 3. Main panel: The light curve of 1-TeV gamma-rays detected by HESS from PSR B1259−63/SS2883 (Aharonian et al. 2005). A reference light curve adopted for derivation of the time profile of non-radiative energy losses of electrons is also shown. The two vertical grey zones correspond to the position of the stellar disc. The somewhat lower flux of gamma-rays at $t \sim 15$ d after the periastron can be associated with the enhanced losses in the disc, and thus may cause more irregular profile of energy losses. Small panel: The reconstructed time profile of adiabatic energy-loss rate derived for the reference TeV light curve shown in the main panel (see the text).

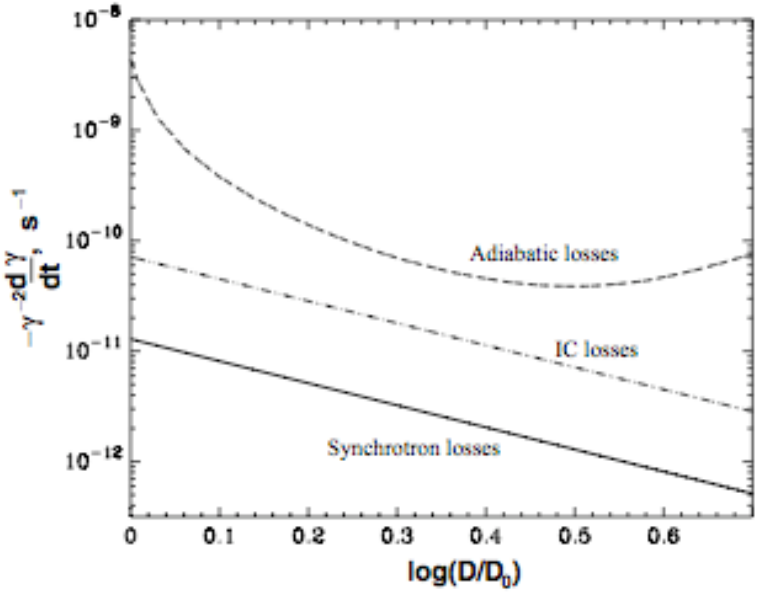

Figure 4. The energy losses for 1-TeV electrons versus the separation distance between the pulsar and the companion star. The solid line is for synchrotron losses for $B = 0.1$ G at periastron, and $B(D) \propto D^{-1}$; the dash–dotted line is for IC losses for blackbody distribution of target photons with temperature $T = 2.3 \times 10^4$ K diluted with coefficient $\kappa = (R_\star/2D)^2$, where $R_\star$ is the radius of the star. The dashed line corresponds to adiabatic losses for the reconstructed time profile shown in Fig. 3 (the small panel).

Khangulyan et al. 2007

Explanation of the TeV lightcurve by a hadronic model

assuming a specific position of the stellar disk the excess of the radio, X- and TeV γ-rays can be explained as result of the entrance of pulsar into the disk …

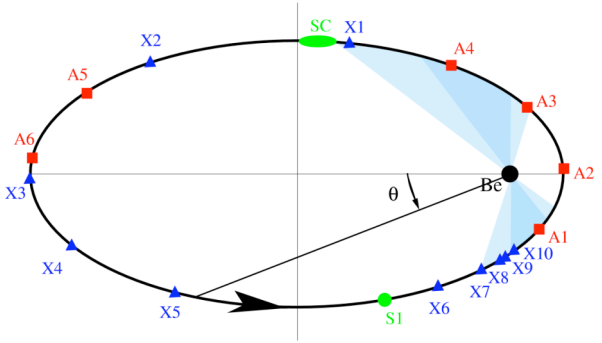

pp interactions responsible for γ-rays?

radio and X-ray – result of the synchratron/IC of low-energy electrons?

Chernyakova, Neronov et al. 2006

but the latest HESS results show appearance of γ-rays before the entrance of the pulsar into the disk…

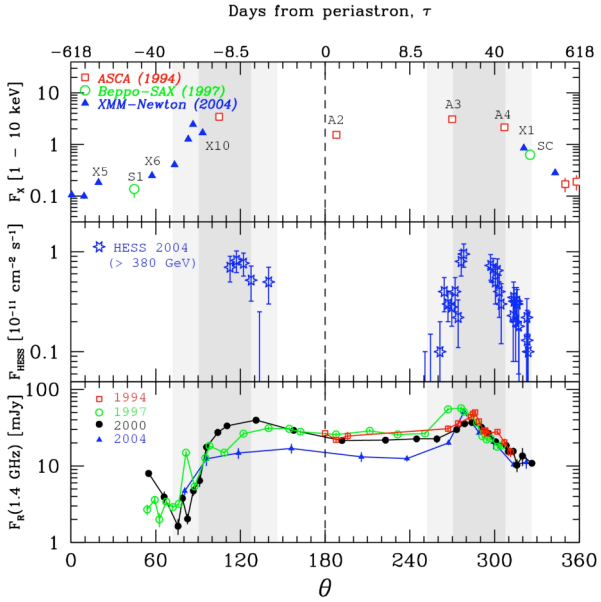

HESS observations of PSR1259-63 in 2007

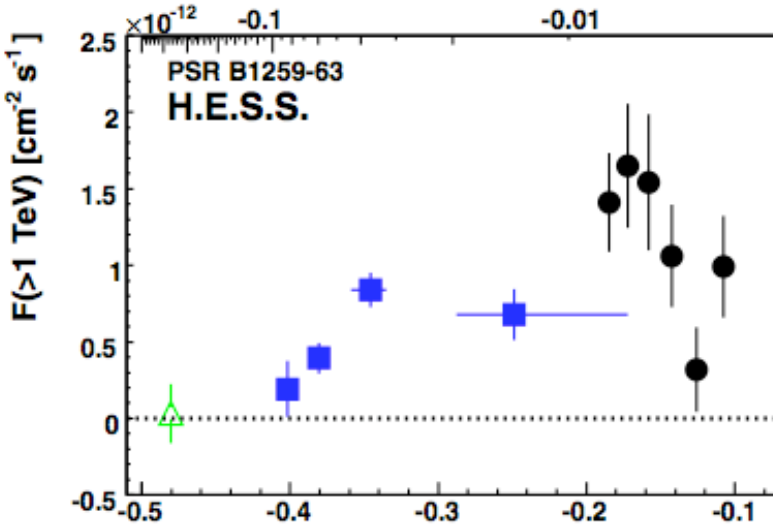

Fig. 5. VHE integrated flux from PSR B1259−63 above 1 TeV as a fu
are shown on the upper horizontal axis. The red vertical line indica
black points are the daily fluxes as measured in 2004. Green empt
squares represent the monthly fluxes taken from the campaign in 20(

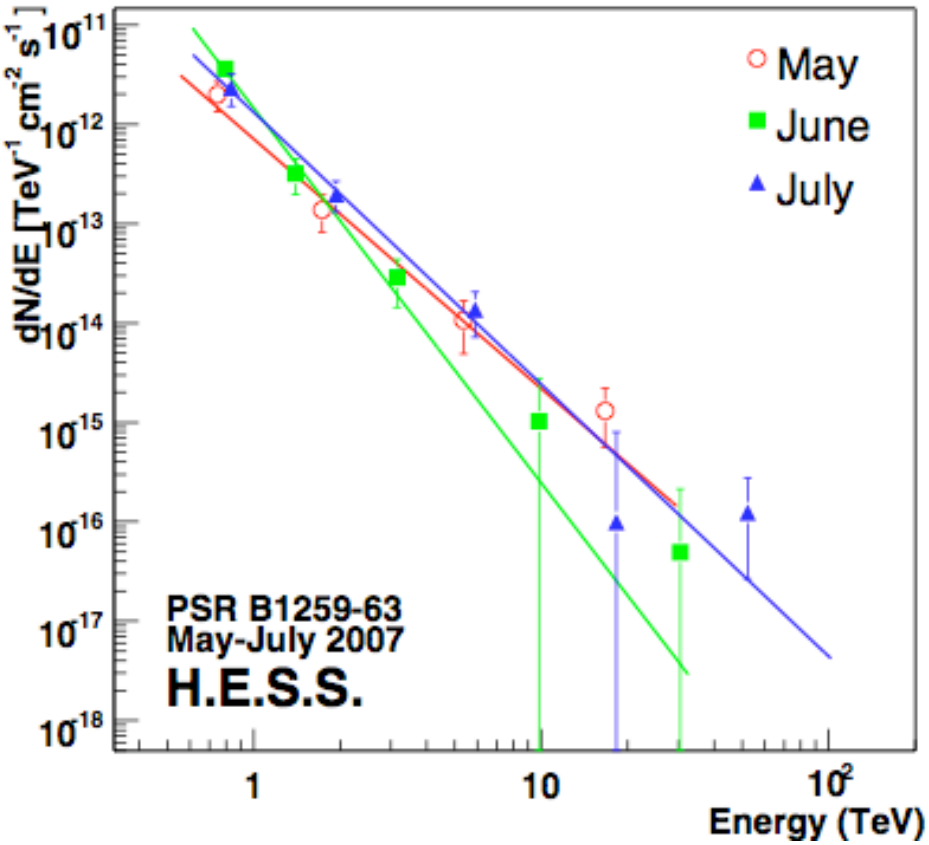

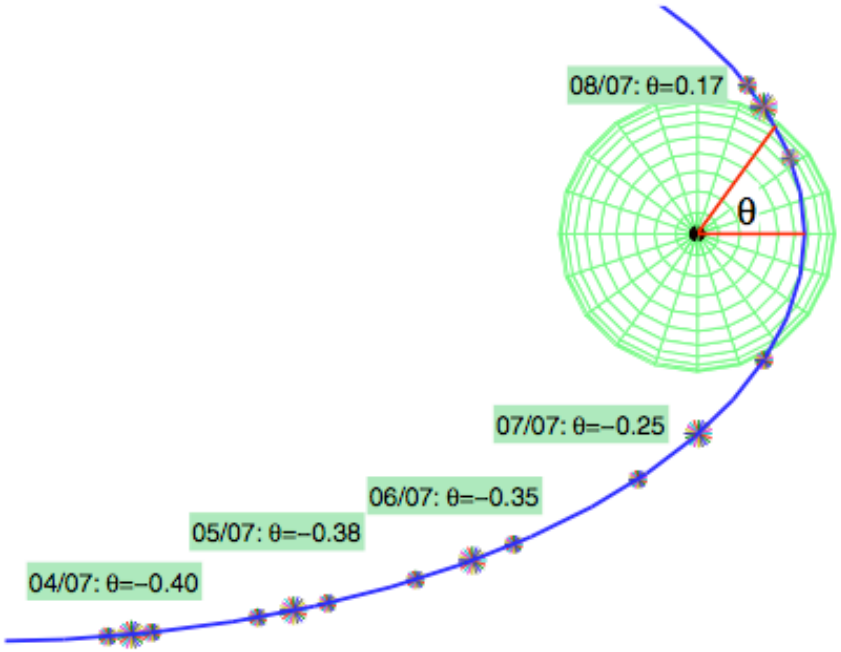

Fig. 6. Top view model sketch for the PSR B1259−63/SS2883 orbit. The black dot represents SS2882 and the circumstellar disc is depicted in green. The pulsar size is exaggerated by a huge factor. The circumstellar disc is assumed to be extended out to 20 stellar radii $R_{\odot}$, as typical for Be stars. The mean pulsar positions for the individual HESS observation periods in 2007 are shown along the orbital trajectory as stars together with the corresponding date and the true anomaly θ (definition indicated by red thin lines). The smaller stars indicate the pulsar position of each period's first and last measurement, respectively. The positive excess of TeV photons in June 2007 at an orbital position of $\theta \approx -0.35$ seems to have occurred far outside the estimated disc crossing phase.

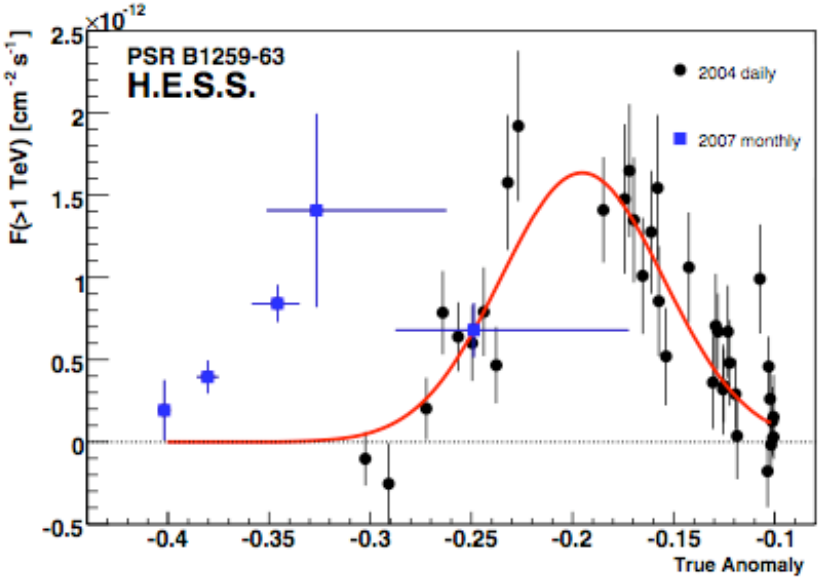

Fig. 7. Fit of the 2004 (black points) integrated flux data above 1 TeV with a Gaussian following Fig. 4 in Chernyakova et al. (2006) in order to determine the location of the circumstellar disc in comparison with fluxes measured in 2007 (blue squares). The 2007 data deviates considerably from the suggested disc density model.

HESS 2007 data disfavour hadronic origin of gamma-rays - good news!

Explanation of the TeV lightcurve within the IC model:

Componization of the Wind

probing the wind Lorentz factor with HESS and GLAST

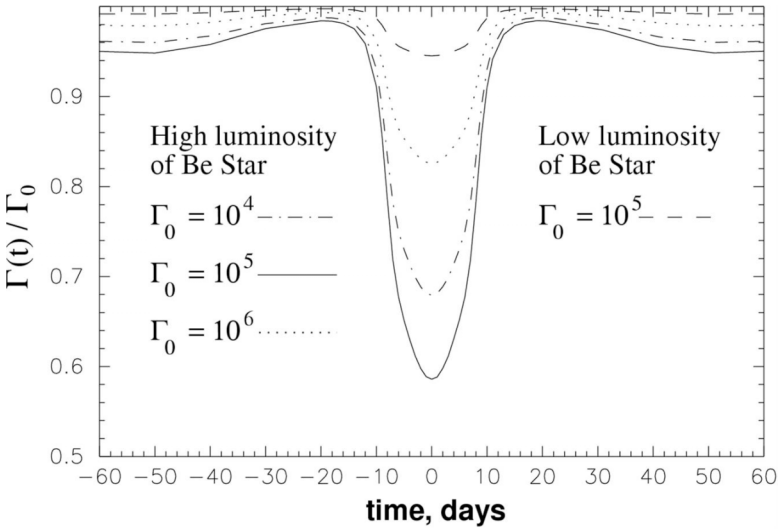

reduction of the Lorentz factor of the electron-positron win ("deacceleration" of the wind)

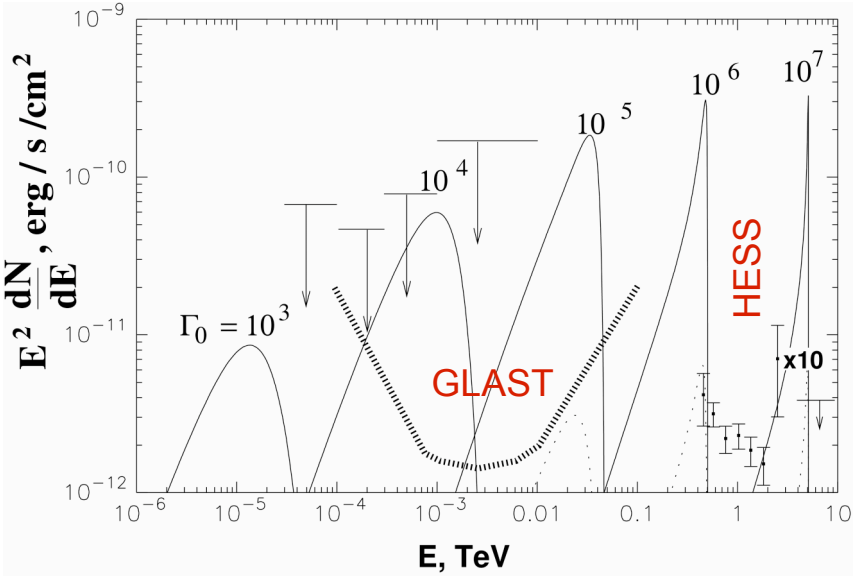

Lorentz factors > 10^6 are excluded by HESS; $\Gamma=10^3$-10^5 range can be probed by GLAST

TeV Gamma Rays From LS5039 and LSI+61 303

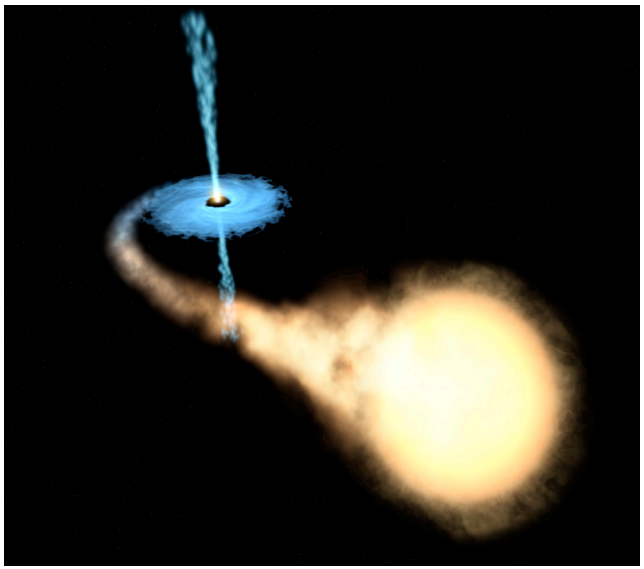

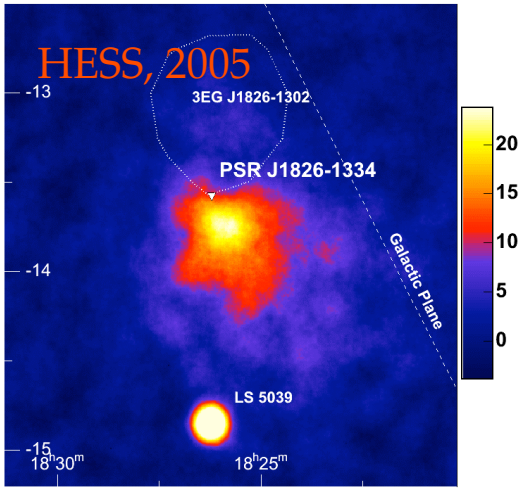

microqusars or binary pulsars?

independent of the answer – particle acceleration is linked to (sub) relativistic outflows

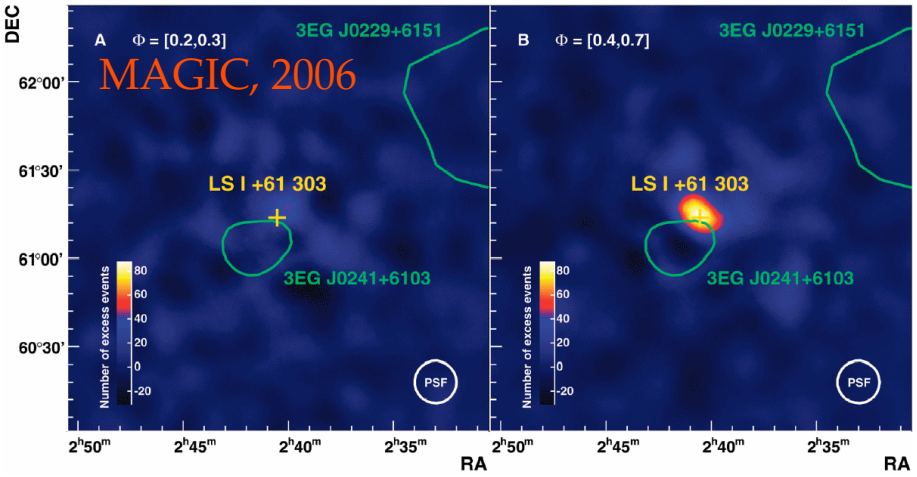

Predicting GeV/TeV γ-rays from μQSOs

(Levinson&Blandford 1995, FA&Atoyan 1998, after the discovery of μQSOs in 1994)

- they are scaled-down versions of AGN, in particular blazars
  no problem with $\delta < 1$; it is compensated by larger L_{Edd}/d^2 $(M_{BH}/d)^2$ in μQSOs is larger, by several orders of magnitude than in BL Lacs)

- relativistic outflows are very (most) effective sites for acceleration of particles to GeV/TeV energies and beyond
  large scale synchrotron jets discovered from mQSOs !

- SSC modeling of GRS 1915 based on R and IR data, and assuming that the electron spectrum extends to >10 TeV predicts detectable IC γ-ray fluxes provided that B-field is somewhat below its equipartiton value
  no strong evidence of TeV gamma-rays from GRS1915

- μQSOs in binary systems with very luminous optical companion stars
  enhanced IC emision because of copious target (starlight)
  we do see TeV gamma-rays from such systems but are these objects μQSOs

- gamma-rays from hadronic interactions ?

  actually we do not need them, but who knows ...

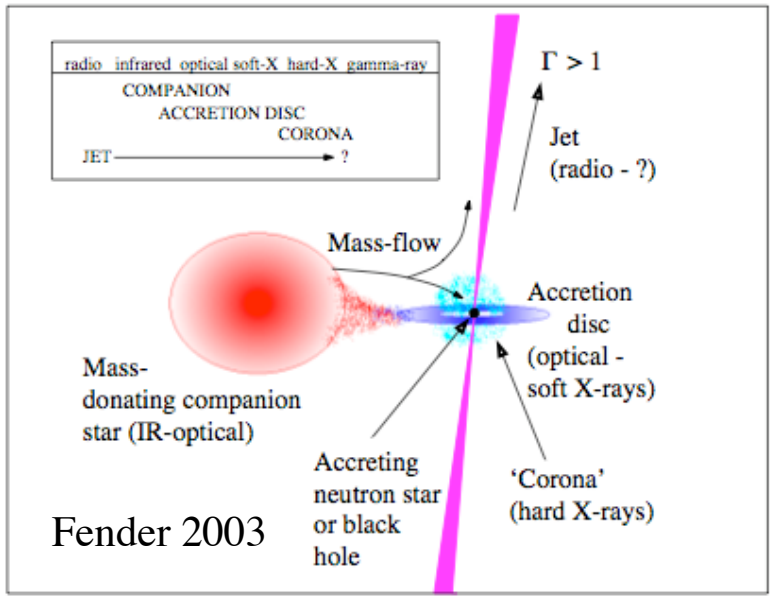

Fender 2003

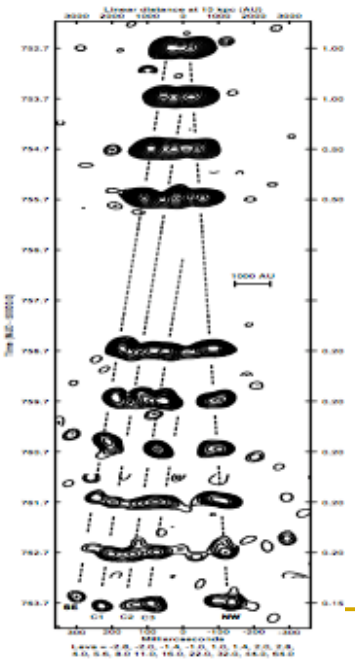

F. Mirabel

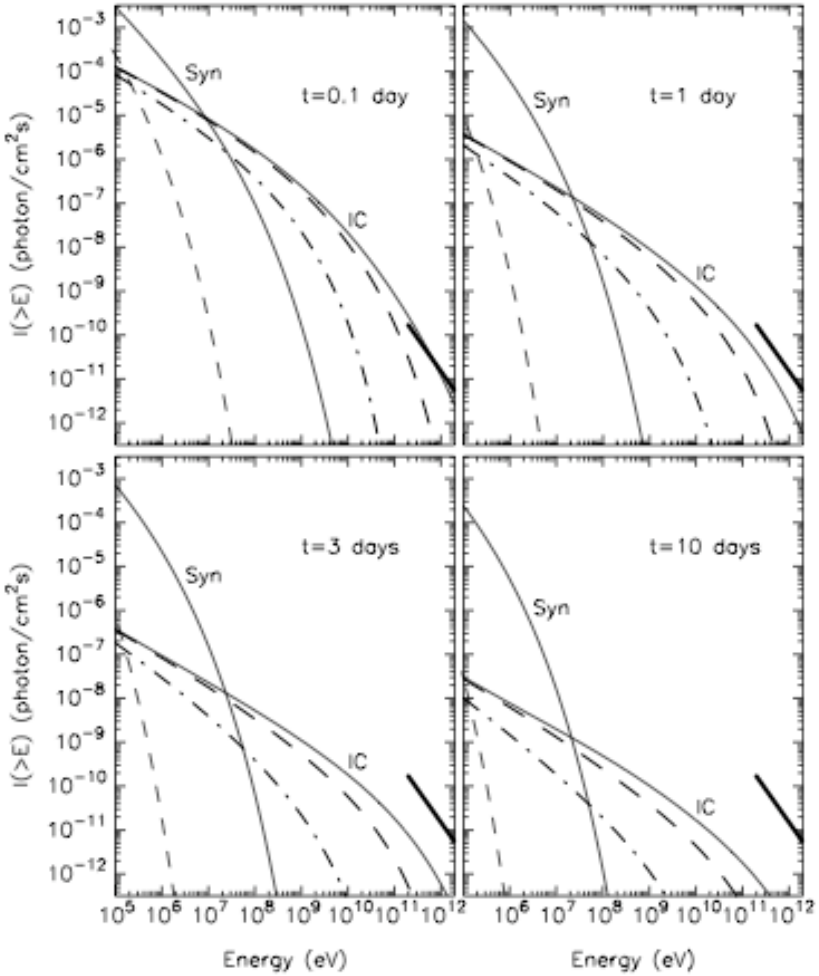

Fig. 7.6 Gamma-ray fluxes expected at different times t during a powerful flare like the 19 March 1994 outburst of GRS 1915+105, calculated for $B_0 = 0.05$ G assuming 3 different exponential cutoff energies: $E_c = 20$ TeV (solid), $E_c = 1$ TeV (dashed), and $E_c = 30$ GeV (dot-dashed). The heavy solid line corresponds to the level of the VHE γ-ray flux of the Crab Nebula. (From Aharonian and Atoyan, 1998b).

LS5039 and LS I +61 303

presence of two basic components for TeV γ-ray production !

- the compact object initiates (through a BH jet or a pulsar wind) acceleration of electrons (protons ?) to energies at least 10 TeV
- 10^{39} erg/s companion star provides seed photons for IC or pγ or dense wind for pp interactions

scenario ? γ-ray production region within (despite $\tau_{\gamma\gamma} >> 1$) and outside the binary system cannot be excluded

periodicity expected ? **yes** – because of periodic variation of the geometry (interaction angle) and density of optical photons – as target photons for IC scattering and γγ absorption, as well as a regulator of the electron cutoff energy E_{cut} ; also because of variation of the B-field, density of the ambient plasma (stellar wind), ...

LS 5039 as a TeV clock with T=3.9078 +/- 0.0015day

[chance probability < 10^{-15}]

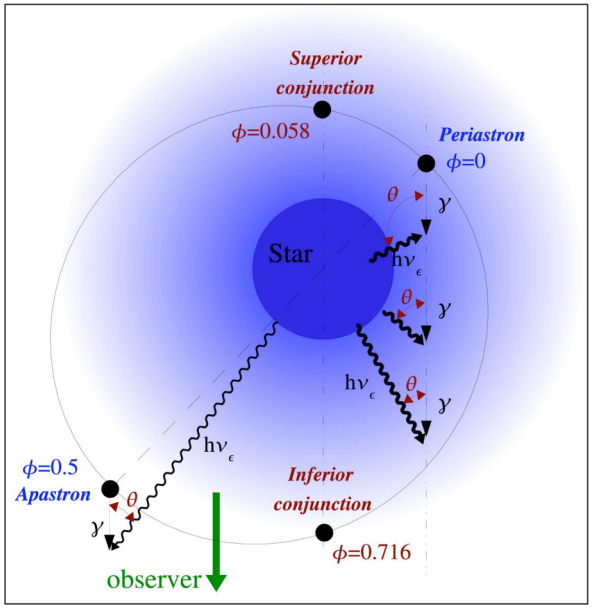

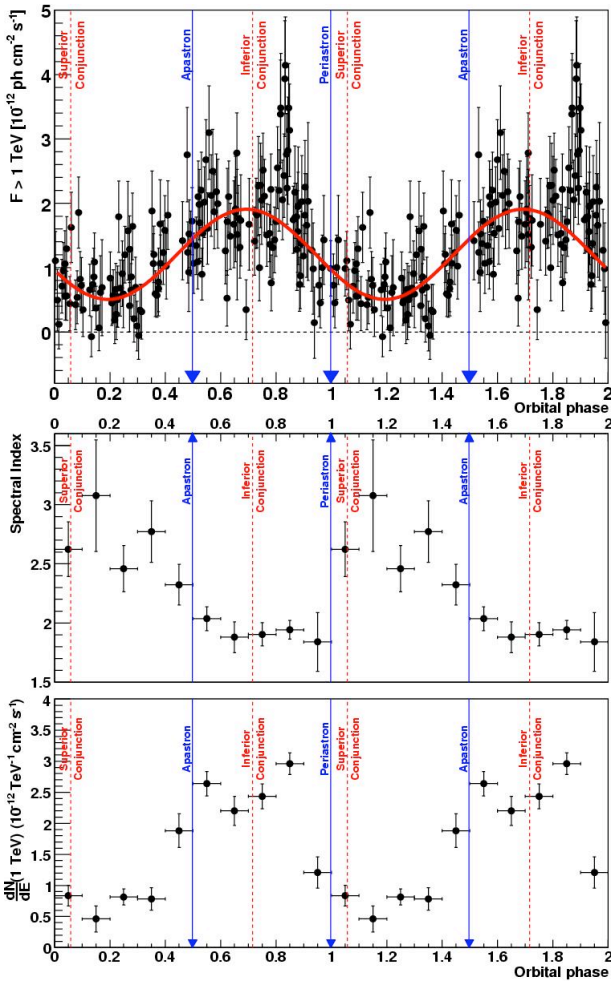

close to inferior conjuction - maximum
close to superior conjuction – minimum

absorption a prime reason for modulation
(Moskalenko95, Böttcher&Dermer06, Dubus06, ...) ?

Period of the system (via Doppler shifted opticl lines) T=3.90603+/-0.00017d

gamma-rays are observed around ϕ=0
(supprerssion expected several orders of magnitude - due to cascading?

strongest absorption below 1 TeV
just opposite dendency is observed !

conclusion? – absorption (alone) cannot explain the observed modulation

main reason for modulation? – variation of E_{max} and/or scattering angle

TeV γ-ray production region?
likely at the edge or even outside the binary system - to avoid significant absorption and allow E_{max} > 10 TeV

➔ BH Jet rather than Pulsar Wind ?

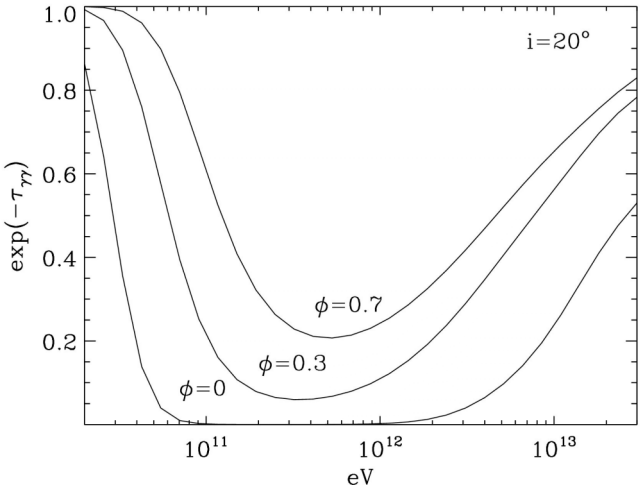

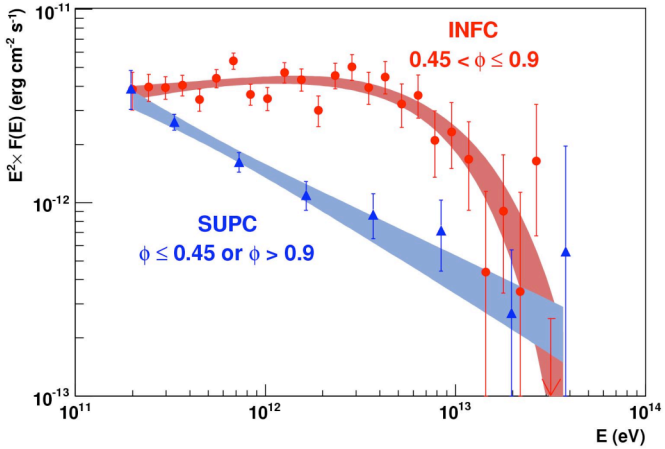

modulated X-ray signal:

explanation? adiabatic loses

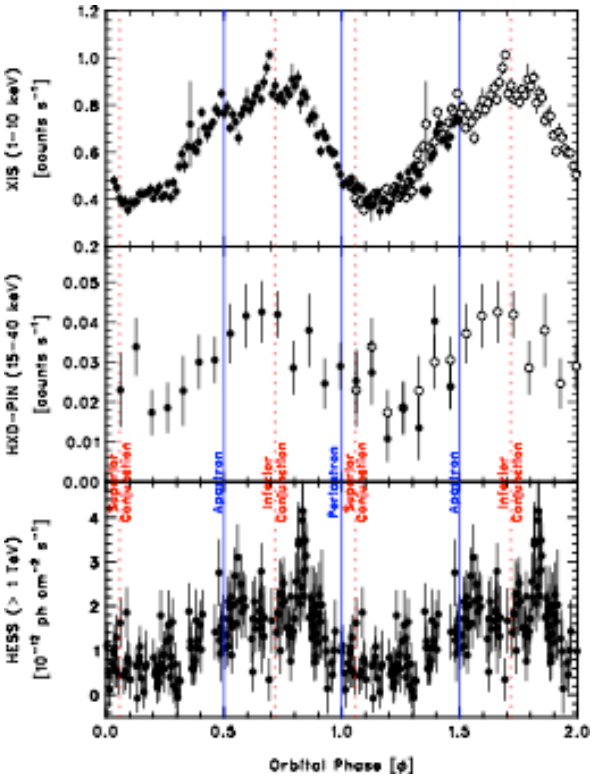

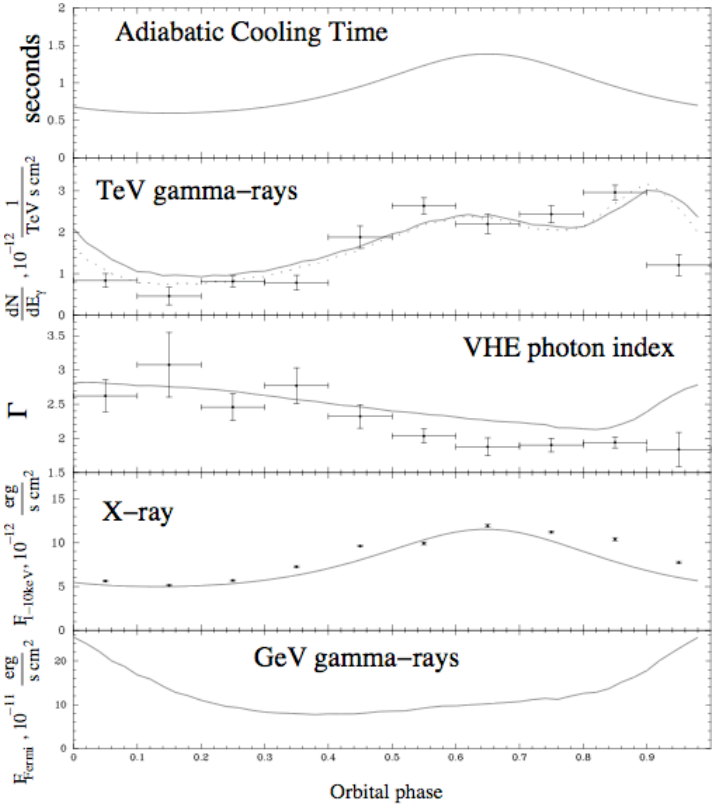

Takahashi et al. 2009

theoretical predictions and recent very recent Fermi results

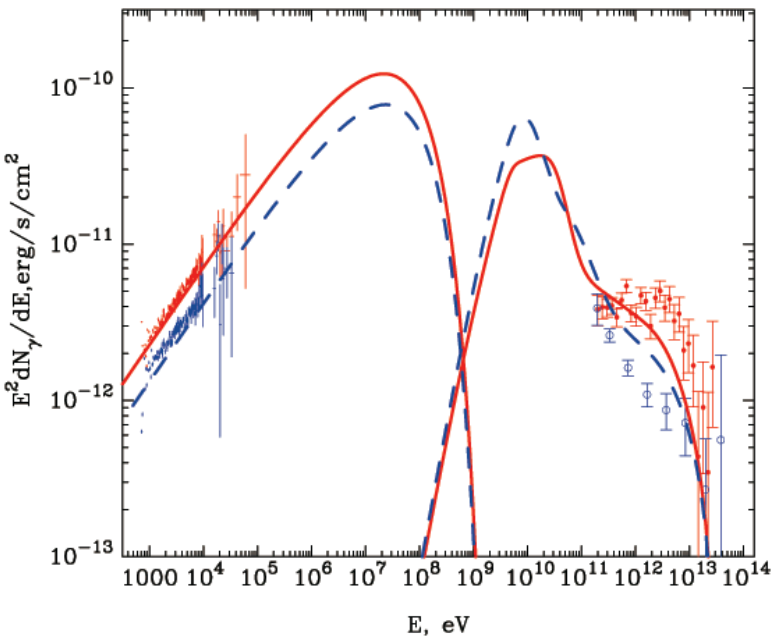

FIG. 7.— Model calculations of the non-thermal radiation spectra of LS 5039, averaged over SUPC (low state) and INFC (high state) orbital phase intervals for $\phi \leq 0.45$, $\phi \geq 0.9$ (SUPC, Blue); and for $\phi = 0.45$–0.9 (INFC,Red). The flux points of *Suzaku* X-ray spectra (1–40 keV band) are reconstructed with the best-fit function with correction for the interstellar absorption. The HESS gamma-ray spectra are taken from Aharonian et.(2006). The calculations were performed for the same model parameters as in Fig. 6

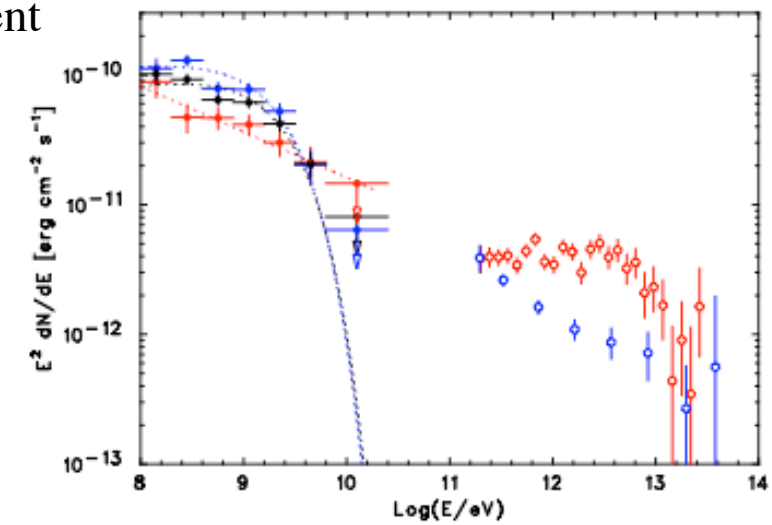

FIG. 3.— Fitted spectrum of LS 5039. Fermi data points are from likelihood fits in each energy bin. The black points (dotted line) represent the phase-averaged *Fermi*/LAT spectrum. The red data points (dotted line) represent the spectrum (overall fit) at inferior conjunction (Phase 0.45–0.9); blue data points (dotted line) represent the spectrum (overall fit) at superior conjunction (Phases, <0.45 and >0.9). Data points above 100 GeV are taken from H.E.S.S. observations (Aharonian et al. 2006); the data from H.E.S.S. are not contemporaneous with *Fermi*, though they do cover multiple orbital periods.

does not agree at 100MeV (slight Doppler shift $\delta \sim 3$ of the synch. component) and low energy cutoff in electron spectrum, $E^* > 10$ GeV) ?

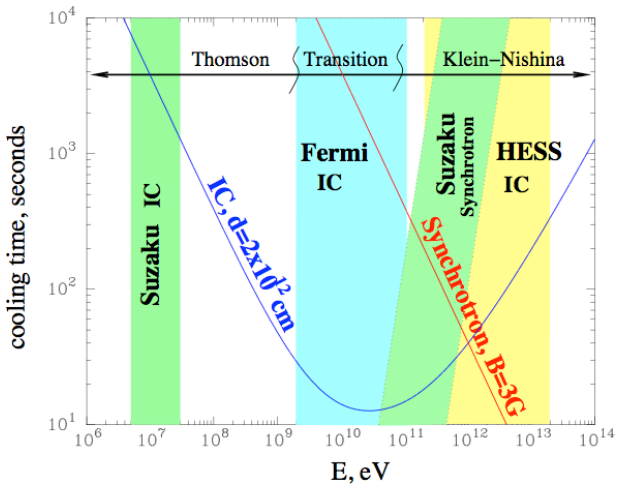

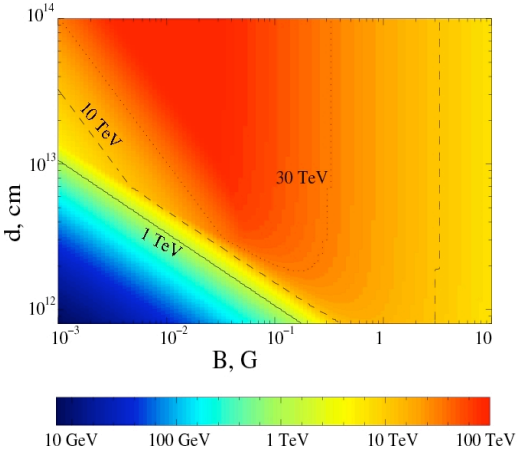

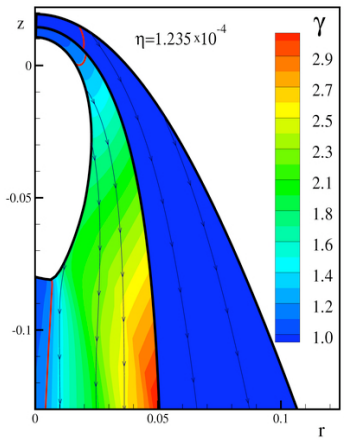

- can electrons be accelerated to > 20 TeV in presence of radiation?

  yes, but accelerator should not be located deep inside the binary system, and even at the edge of the system $\eta < 10$

- does this excludes the model of "binary pulsar"

  yes, unless the interaction of the pulsar and stellar winds create a relativistic bulk motion of the shocked material (it is quite possible)

Cascades? (Heidelberg, Barcelona,

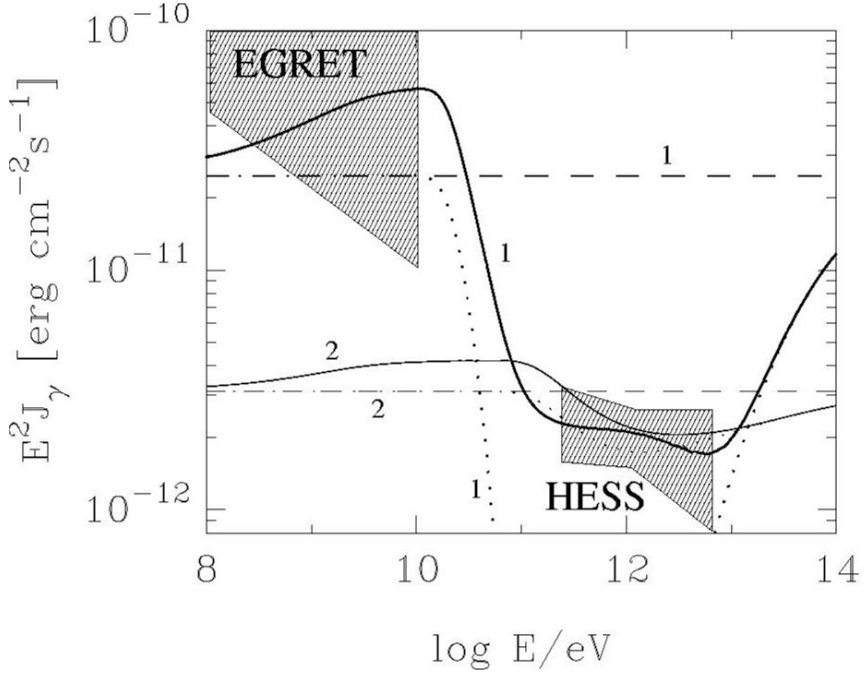

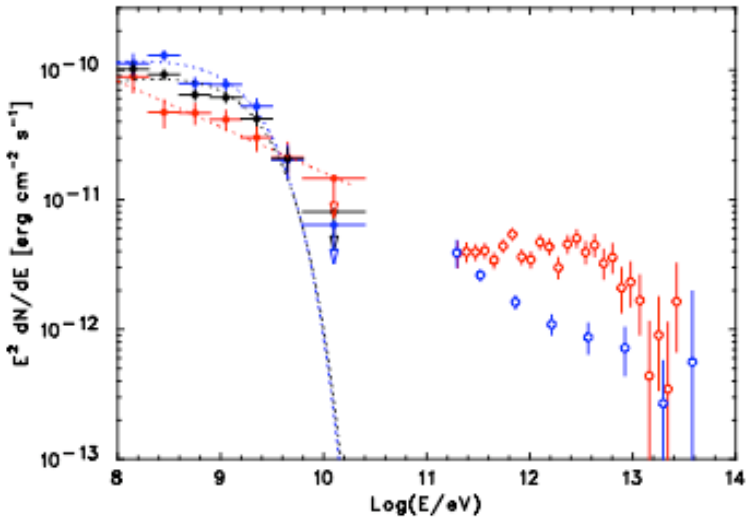

FIG. 3.— Fitted spectrum of LS 5039. Fermi data points are from likelihood fits in each energy bin. The black points (dotted line) represent the phase-averaged *Fermi*/LAT spectrum. The red data points (dotted line) represent the spectrum (overall fit) at inferior conjunction (Phase 0.45–0.9); blue data points (dotted line) represent the spectrum (overall fit) at superior conjunction (Phases, <0.45 and >0.9). Data points above 100 GeV are taken from H.E.S.S. observations (Aharonian et al. 2006); the data from H.E.S.S. are not contemporaneous with *Fermi*, though they do cover multiple orbital periods.

work in progress, but it seems the γ-ray production region should not be located very deep inside the system to avoid the observed GeV/TeV < 2-5 ratio

HESS J0632+057: *a new TeV binary?*

J. Skilton et al. 2009

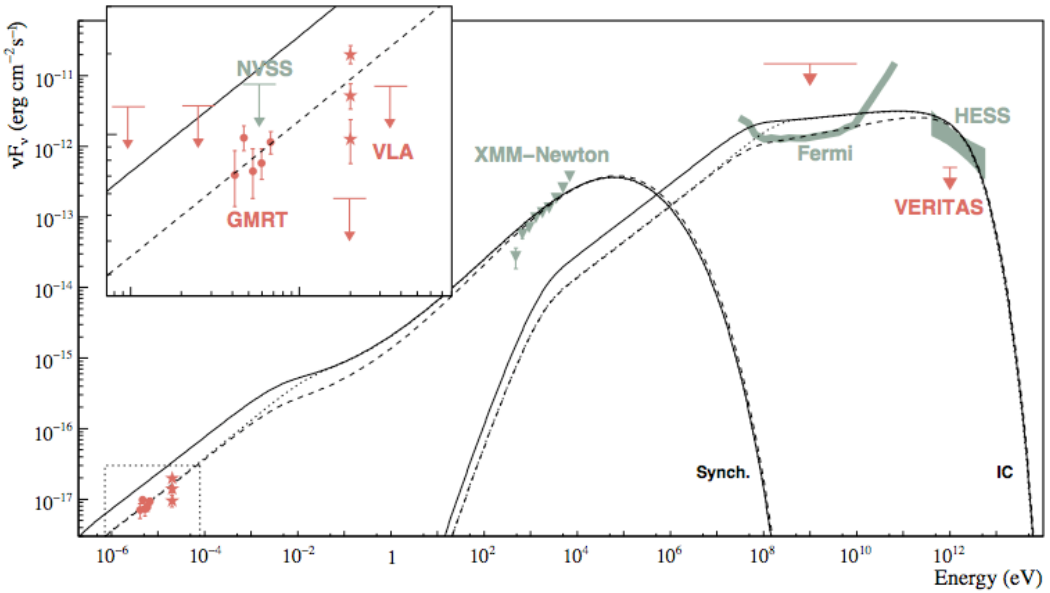

Figure 4. SED of HESS J0632+057 adapted from (Hinton et al. 2009), with new data shown in red. The GMRT measurements have been plotted slightly offset from their observing frequency for clarity. The data are compared to a one-zone model of non-thermal emission from electrons cooling in the radiation and magnetic fields within a few AU of MWC 148. The three model curves show an injection electron spectral index 2.0 (solid lines) and 1.9 (dashed lines), and an index of 2.0 but with a low energy cut-off at 2 GeV rather than 1 GeV (dotted line). See Hinton et al. (2009) for more details. An upper limit for GeV emission from HESS J0632+057 based on three months of Fermi observations (Abdo et al. 2009) and the 1 year Fermi sensitivity curve are shown. **An approximate energy flux limit from VERITAS is also shown (Acciari et al. 2009), highlighting the variable nature of the TeV emission.**

HESS collab. 2007

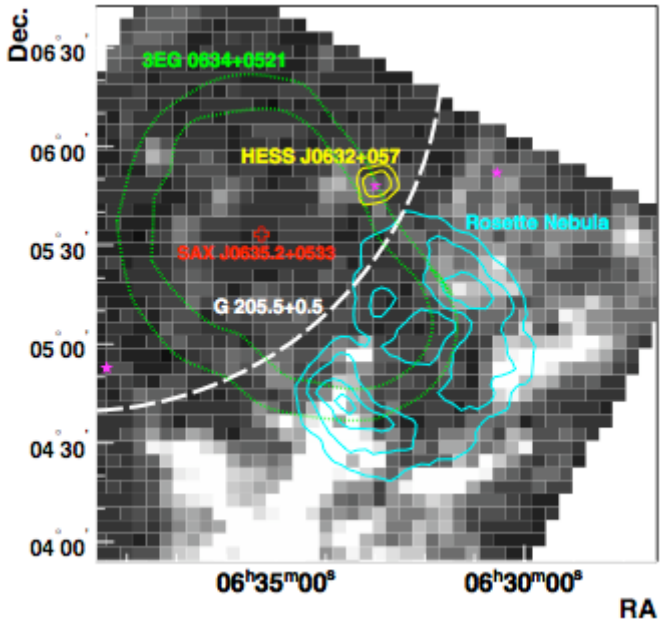

(i) a point TeV source, (ii) possible hard-spectrum variable X-ray source and Be star counterparts, (iii) evidence of long-term very high energy gamma-ray flux variability (VERITAS) - good reasons to assume/claim a newly detected TeV/X-ray binary.